Demultiplexer based on an off-axis holographic lens with low monochromatic aberrations

Sensen Li (李森森)[1*], Shou Liu (刘 守)[2], Xiangsu Zhang (张向苏)[2], and Xuechang Ren (任雪畅)[2]

[1] *Department of Electronic Engineering, Xiamen University, Xiamen 361005, China*

[2] *Department of Physics, Xiamen University, Xiamen 361005, China*

[*] *Corresponding author: sensenli@xmu.edu.cn*

Received February 28, 2011; accepted April 28, 2011; posted online June 30, 2011

A novel scheme is proposed, in which the aberrations in the off-axis holographic lenses used as demultiplexers are reduced to a low enough level for relatively small channel spacing. The scheme includes optimizing the recording and reconstruction geometries and collimating the reconstruction wave with a gradient-index lens. A demultiplexer operated in the 1 550-nm band with 5-nm channel spacing and $-\infty$-dB crosstalk is obtained using the scheme. The channel spacing can be decreased to 2 nm by etching the cladding of the output fibers to a smaller size.

OCIS codes: 060.1810, 090.2890, 090.1000.

doi: 10.3788/COL201109.090603.

Wavelength-division multiplexing (WDM) is an effective technique to increase the information capacity of fiber-optic networks. Demultiplexers (DEMUXs) are essential devices in WDM systems. Many types of DEMUXs have been proposed[1−3]. Among these, the diffraction-grating type has the special advantage of being scalable, such that lower channel count devices can be upgraded to higher count devices simply by installing more fibers[4]. Off-axis holographic lenses (OHLs) are ideal candidates for DEMUXs of this type due to their functions of dispersion and focus in a single element. OHL-based devices[5−7] can achieve simplification in alignment and improvement in stability because few auxiliary elements are required. An additional advantage is that surface-relief OHLs are suitable for mass production by replication techniques[8], thereby leading to devices with lower cost.

When OHLs are used as DEMUXs, they suffer from monochromatic aberrations because of the different wavelengths for recording and reconstruction. The consequent blurred focal spots of OHLs cause serious cross talk, thereby restricting the channel spacing reduction of DEMUXs if aberrations are high. Therefore, reducing the aberrations of OHLs is a crucial problem. Ishii *et al.* proposed the scheme of using an optimum aspheric wave diffracted from a computer-generated hologram as object wave, obtaining a DEMUX operated near 800 nm with a 20-nm channel spacing and $-\infty$-dB crosstalk[6]. Ren *et al.* proposed another scheme of choosing certain geometries that can simplify the aberration coefficients, obtaining a DEMUX operated near 1 100 nm with about 25-nm channel spacing and −10-dB crosstalk[7]. However, neither scheme can make the aberrations of the OHL low enough for relatively small channel spacing.

In this letter, we propose the scheme of optimizing the recording and reconstruction geometries and then collimating the reconstruction wave with a gradient-index (GRIN) lens to make the aberrations of OHLs low enough for relatively small channel spacing. A DEMUX operated in the 1 550-nm band with a 5-nm channel spacing and $-\infty$-dB crosstalk is obtained. Channel spacing of 2 nm can be achieved by etching the cladding of the output fibers to a smaller size.

OHLs are actually point source holograms. An OHL located in the XOY plane, with the center at the origin and the optical geometry arranged in the XOZ plane for both recording and reconstruction, can have a real image point in the XOZ plane with the third-order aberrations given by[9]

$$\phi = -S\left(x^2+y^2\right)^2/8 + Cx\left(x^2+y^2\right)/2 - Ax^2/2, \quad (1)$$

where S, C, and A are the coefficients of the spherical aberration, coma, and astigmatism, respectively. Equation (1) demonstrates that low aberration coefficients and a small irradiation region on the OHL can both reduce the third-order aberrations.

Surface-relief gratings (SRGs) with an even-symmetric profile can have a high (>85%) diffraction efficiency (DE)[10]. Therefore, a divergent spherical object wave and a plane reference wave with symmetrical incidence were chosen to record OHLs on a photoresist. In addition, the spherical object wave came from a point source located at a distance much farther than the recording region. Thus, the microstructures of OHLs can be regarded as sinusoidal SRGs. To obtain a small irradiation region, the reconstruction wave was collimated by a GRIN lens. In such a case, the location of the real image point is given by[9] $\sin\alpha_{\rm I} = \sin\alpha_{\rm C} - 2\mu\sin\alpha_{\rm O}$ and $R_{\rm I} = -R_{\rm O}/\mu$; the aberration coefficients in Eq. (1) are expressed as[9]

$$\begin{aligned} S &= \mu\left(\mu^2-1\right)/R_{\rm O}^3 \\ C &= \left(\mu/R_{\rm O}^2\right)\left[\left(2\mu^2-1\right)\sin\alpha_{\rm O} - \mu\sin\alpha_{\rm C}\right] \\ A &= \left(\mu/R_{\rm O}\right)\left[\left(\sin\alpha_{\rm C} - 2\mu\sin\alpha_{\rm O}\right)^2 - \sin^2\alpha_{\rm O}\right] \end{aligned}, \quad (2)$$

where $\sin\alpha_Q = x_Q/R_Q$, x_Q, and R_Q are the coordinates and distance from the origin of the point Q (Q=O, R, C, I), respectively; O, R, C, and I denote object, reference source, reconstruction source, and image, respectively; a positive R_Q represents a divergent wave, and a

 © 2011 Chinese Optics Letters

negative R_Q a convergent wave; $\mu = \lambda_C/\lambda_O$, λ_C and λ_O are the reconstruction and recording wavelengths, respectively. The equations shown above show that aberration coefficients can be minimized by optimizing the recording and reconstruction geometries.

Equation (2) indicates that conditions minimizing the three aberration coefficients are different. Specifically, a large R_O can minimize S to near zero, whereas the following two conditions

$$\sin\alpha_C = (2\mu - 1/\mu)\sin\alpha_O \tag{3}$$

and

$$\sin\alpha_C = (2\mu \pm 1)\sin\alpha_O \tag{4}$$

can minimize C and A to zero, respectively. Therefore, OHLs capable of high DE were analyzed as samples to compare the influence of the three aberrations on the focusing function of OHLs. To investigate the blurred focal spots of the OHL due to the three aberrations, ray aberrations of the real image point were analyzed. These are expressed as[11]

$$\begin{aligned} x'_I - x_I &= (R_O/\mu)(\partial\phi/\partial x) \\ y'_I - y_I &= (R_O/\mu)(\partial\phi/\partial y) \end{aligned}, \tag{5}$$

where (x_I, y_I) and (x'_I, y'_I) are coordinates of the Gaussian image point and the point of intersection of an aberrated ray with the Gaussian image plane, respectively.

For OHLs capable of a high DE, the reconstruction wave should occur at the first Bragg angle given by[10]

$$\theta_B = \arcsin\left[\lambda_C/(2\bar{\Lambda})\right], \tag{6}$$

where $\bar{\Lambda} = \lambda_O/(2\sin\theta)$, $\bar{\Lambda}$ is the average period of OHL, and θ is the incident angle of the two recording waves. If the geometries shown in Fig. 1 are used for recording and reconstruction, substituting $\alpha_O = -\theta$ and $\alpha_C = -\theta_B$ into Eq. (6) yields

$$\sin\alpha_C = \mu\sin\alpha_O. \tag{7}$$

Simulations performed with the GSolver software revealed that OHLs showed a high DE for any incident polarization state at certain groove depths ($\leqslant 10\lambda_C$) when $\bar{\Lambda} \leqslant 1.4\lambda_C$. In addition, $|\sin\alpha_C| \leqslant 1$ and $|\sin\alpha_I| \leqslant 1$ must be met. When $\lambda_O = 458$ nm and $\lambda_C = 1\,550$ nm, $6.1^\circ \leqslant \theta \leqslant 17.1^\circ$ should be observed.

As an example, ray aberrations of OHLs capable of a high DE and with $\theta = 14.0^\circ$ and $R_O = 10.0$ cm, are presented in Fig. 2. Astigmatism is the main cause of enlargement of the focal spot; the influence of a coma is much smaller, and the influence of a spherical aberration can be neglected. This implies that 10.0 cm is large enough for R_O to minimize S to near zero. Equation (4) is somewhat similar to Eq. (3) when the minus sign is selected, therefore the two conditions

$$\begin{aligned} &R_O \geqslant 10.0\ \text{cm} \\ &\sin\alpha_C = (2\mu - 1)\sin\alpha_O \end{aligned} \tag{8}$$

were chosen to minimize aberration coefficients. The results are given by

$$\begin{aligned} &S \approx 0 \\ &C = \mu(\mu - 1)\sin\alpha_O/R_O^2, \\ &A = 0 \end{aligned} \tag{9}$$

which are much lower than those in Ref. [7]. Given that $|\sin\alpha_C| \leqslant 1$ and $|\sin\alpha_I| \leqslant 1$ must be met, $\lambda_O = 458$ nm and $\lambda_C = 1\,550$ nm should yield $\theta \leqslant 9.9^\circ$.

To obtain adequate spaces to install the output fibers, and make the real image wave couple with output fibers, the two inequalities given by

$$\begin{aligned} &|R_I| \cdot |(\mathrm{d}\alpha_I/\mathrm{d}\lambda_C)\,\delta\lambda_C| \geqslant 2b \\ &\arctan\left(D_{\mathrm{eff}}/|2R_I\cos\alpha_C|\right) \leqslant \theta_a \end{aligned} \tag{10}$$

should be met in the design of OHLs, where $\delta\lambda_C$ is channel spacing, D_{eff} is the effective diameter of the GRIN lens, and b and θ_a are the cladding radius and the acceptance angle of output fibers, respectively.

An OHL with minimized aberration coefficients (called OHL1) was fabricated on a CHP-C positive photoresist using a 458-nm laser light and the geometry shown in Fig. 1(a). For comparison, another OHL capable of high DE (called OHL2) was also fabricated. Both OHLs were designed for channel spacing of 5 nm and had the same recording geometry parameters of $\theta = 9.0^\circ$

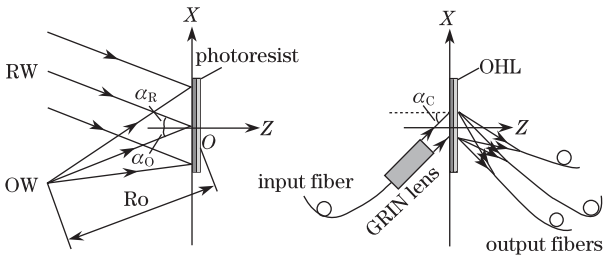

(a) (b)

Fig. 1. Geometries of (a) recording and (b) reconstruction for OHL. OW and RW denote object wave and reference wave, respectively.

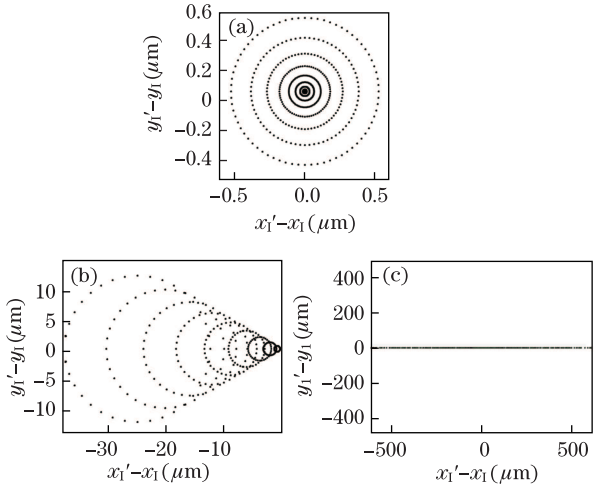

Fig. 2. Ray aberrations of an OHL capable of high DE and with recording geometry parameters of $\theta = 14.0^\circ$ and $R_O = 10.0$ cm. (a) Spherical aberration, (b) coma, and (c) astigmatism. (x_I, y_I) and (x'_I, y'_I) are the coordinates of the Gaussian image point and the point of intersection of an aberrated ray with the Gaussian image plane, respectively.

and $R_{\rm O}$ = 12.5 cm. Then, DEMUXs constituted by OHL1 and OHL2, called DEMUX1 and DEMUX2, respectively, were tested using an amplified spontaneous emission (ASE) source and an optical spectrum analyzer. In both DEMUXs, the OHL was arranged in a similar geometry as that shown in Fig. 1(b): the input and output fibers were standard single-mode fibers; the wave from the ASE source was collimated by a GRIN lens ($D_{\rm eff}$ = 1.2 mm) and used as a reconstruction wave. The reconstruction geometry parameters were $\alpha_{\rm C1} = -64.5°$, $\alpha_{\rm I1} \approx 9.0°$, and $R_{\rm I1} \approx -3.7$ cm for OHL1; and $\alpha_{\rm C2} = -32.0°$, $\alpha_{\rm I2} \approx 32.0°$, and $R_{\rm I2} \approx -3.7$ cm for OHL2. The average spatial separations of adjacent output fibers for DEMUX1 and DEMUX2 were about 175 and 190 μm, respectively.

The transmission spectra of DEMUX1 and DEMUX2 are shown in Fig. 3. Three channels with center wavelengths of 1 545, 1 550, and 1 555 nm were demonstrated as examples. The adjacent channel crosstalks of DEMUX1 and DEMUX2 were $-\infty$ dB (ignoring background crosstalk) and about -18 dB, respectively. The blurred focal spot of OHL1 due to the third-order aberrations was much smaller than that of OHL2 (Fig. 4); therefore, much less crosstalk was obtained by DEMUX1. The adjacent channel spectra of DEMUX1 were well separated for channel spacing of 5 nm; thus, smaller channel spacing can be achieved by DEMUX1. If adequate spaces are available, in which to install output fibers, the channel spacing of DEMUX1 can be decreased to 2 nm without increasing the crosstalk. This can be realized by etching the cladding of the output fibers to a smaller size. The results of less crosstalk and smaller channel spacing indicate that DEMUX1 demonstrated a better performance.

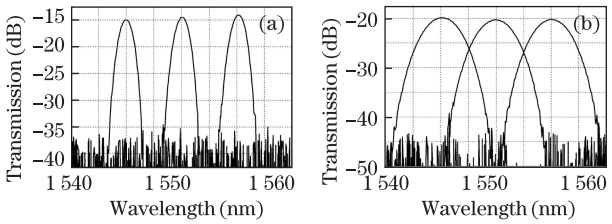

Fig. 3. Transmission spectra of (a) DEMUX1 and (b) DEMUX2. DEMUX1 is constituted by OHL1, and DEMUX2 was constituted by OHL2.

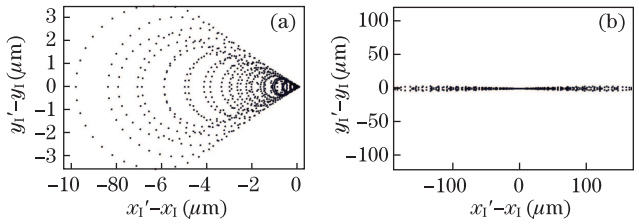

Fig. 4. Ray aberrations of (a) OHL1 and (b) OHL2. OHL1 had minimized aberration coefficients, whereas OHL2 is capable of high DE. They have the same recording geometry parameters of $\theta = 9.0°$and $R_{\rm O} = 12.5$ cm.

The average channel insertion loss (IL) of DEMUX1 was 14.5 dB. The IL included mainly the diffraction loss of OHL1 and the coupling loss of output fibers. The DE of OHL1 was measured to be about 10% using ASE source, implying that OHL1 has the diffraction loss of about 10 dB. Simulation by GSolver revealed that the DE of OHL1 can be improved to 33% by precisely controlling the groove depth, reducing the IL to 9.3 dB. Further reduction of the IL is possible by improving the geometry optimization process of OHLs with grating-matching technique[12], resulting in OHLs with both high DE and low aberrations. Using thermally-diffused expanded core fibers or multi-mode fibers as output fibers to reduce coupling loss can also reduce the insertion loss further.

In conclusion, a novel scheme of reducing aberrations of OHLs used as DEMUXs is proposed. The scheme includes optimizing the recording and reconstruction geometries and collimating the reconstruction wave with a GRIN lens. A DEMUX operated in the 1 550 nm band with 5-nm channel spacing and $-\infty$-dB crosstalk is obtained using the proposed scheme. The channel spacing can be decreased to 2 nm by etching the cladding of the output fibers to a smaller size. These results show that the scheme can make aberrations of OHLs low enough for relatively small channel spacing.

This work was supported by the "985 Project" of Xiamen University and the National Natural Science Foundation of China (No. 50802080). The authors wish to thank Professor X. Dong, Engineer Z. Xie, and Dr. J. Zhou for their assistance in obtaining transmission spectra of demultiplexers presented in this letter.

References

1. D. K. Mynbaev and L. L. Scheiner, *Fiber-Optic Communications Technology* (Prentice Hall, New Jersey, 2001).
2. L. Wosinski, L. Liu, N. Zhu, and L. Thylen, Chin. Opt. Lett. **7,** 315 (2009).
3. C. Liu, Z. Tang, H. Dong, D. Song, Z. Luo, X. Ling, and S. Cao, Chin. Opt. Lett. **8,** 761 (2010).
4. J. Qiao, "Dense wavelength division multiplexing (DWDM) for optical networks", PhD. Thesis (University of Texas at Austin, 2001).
5. J. L. Horner and J. E. Ludman, Appl. Opt. **20,** 1845 (1981).
6. Y. Ishii and T. Kubota, Appl. Opt. **32,** 4415 (1993).
7. X. Ren, Sh. Liu, X. Zhang, and S. Li, Phys. Lett. A **354,** 243 (2006).
8. X. Ren, Sh. Liu, X. Zhang, and S. Li, Proc. SPIE **6832,** 68322M (2007).
9. E. B. Champagne, J. Opt. Soc. Am. **57,** 51 (1967).
10. M. G. Moharam and T. K. Gaylord, J. Opt. Soc. Am. **72,** 1385 (1982).
11. M. Born and E. Wolf, *Principles of Optics* (Cambridge Univ. Press, Cambridge, 1999).
12. H. C. Pedersen and C. Thirstrup, Appl. Opt. **43,** 1209 (2004).